Catalysis Science & Technology

ROYAL SOCIETY OF CHEMISTRY

PAPER

Published on 16 July 2026

Cite this: DOI: 10.1039/d6cy00727a

Mechanistic insight into the formation of aromatics during the MTO process in H-SSZ-13 from DFT calculations

Philipp N. Plessow*[a] and Felix Studt *[ab]

Received 29th May 2026,
Accepted 8th July 2026

DOI: 10.1039/d6cy00727a

rsc.li/catalysis

Aromatics play a key role in the methanol-to-olefins process, both as a co-catalyst for the production of short chain olefins and as a key reaction intermediate towards coke formation, but mechanistic details on how aromatics form are still scarce. Here, we investigate all reaction steps from olefins towards benzene in H-SSZ-13 using density functional theory (DFT) calculations. We find that the rate determining step is likely given by the oxidation of an olefin through hydrogen transfer (HT) reactions, while the subsequent reaction steps of isomerization, cyclization and further oxidation of cyclic olefins are for the most part associated with lower reaction barriers, with the exception of the cyclization of hexadiene, for which cyclization and initial diene formation have similar barriers. Importantly, the key step of oxidation of olefins either through the formaldehyde route or *via* HT of longer chain olefins has barriers on the order of 180 kJ mol^{-1} at 673 K and is thus comparable to those typically found for the methylation of olefins as well as cracking of larger olefins, suggesting that the extent to which the olefin cycle branches towards aromatics formation depends on a delicate balance of the type of olefins formed as well as the Brønsted acid site, but also on the availability of formaldehyde.

Introduction

The catalytic conversion of methanol to olefins (MTO), hydrocarbons (MTH), aromatics (MTA) and jet fuel (MTJ) utilizing acidic zeotype catalysts is attracting growing interest as this production could be based on non-oil and even renewable resources.[1–7] The formation of aromatics is particularly interesting in this aspect for a variety of reasons. Aromatics, especially benzene, toluene and xylenes (BTX) are important base molecules for the chemical industry, while larger aromatics are an important component of jet fuel.[8,9] Furthermore, aromatics play an important role in the catalytic MTO process as they act as co-catalysts within the microporous framework of zeolites constituting the so-called aromatic cycle of the hydrocarbon pool (HPC) mechanism.[10–12] Importantly, they are also key precursors for coke formation, the main cause of catalyst deactivation.[13–18]

Both the role and formation of aromatic molecules during the above mentioned processes have therefore been studied extensively, both experimentally[8,19–30] and theoretically.[31–37] The formation of (substituted) benzene from methanol and olefins concurs with a reduction of the H/C ratio of the olefin, hence its oxidation. It thus requires the removal of hydrogen through hydrogen transfer (HT) processes,[29] with *e.g.* olefins acting as hydrogen acceptors that are hence

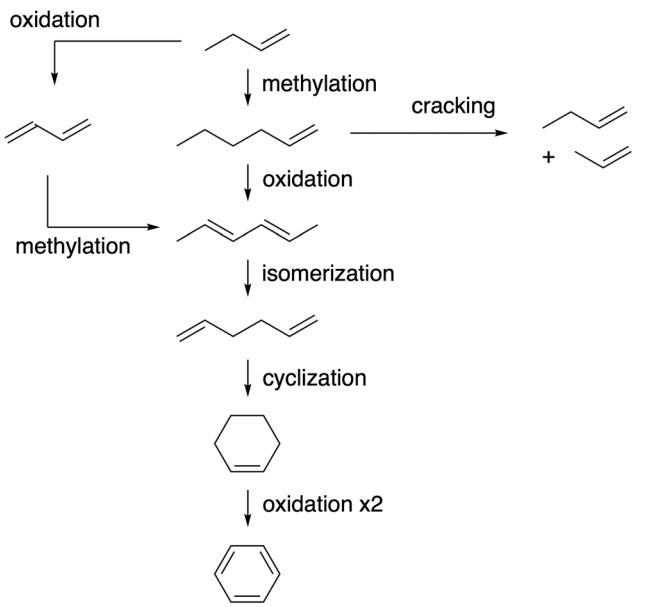

Scheme 1 Schematic presentation of the conversion of olefins to aromatics through the formation of dienes *via* oxidation and isomerization.

[a] *Institute of Catalysis Research and Technology, Karlsruhe Institute of Technology, 76344 Eggenstein-Leopoldshafen, Germany. E-mail: philipp.plessow@kit.edu*
[b] *Institute for Chemical Technology and Polymer Chemistry, Karlsruhe Institute of Technology, 76131 Karlsruhe, Germany*

transformed to hydrocarbons (see Scheme 1). Although no classical oxidant like O_2 is involved, the oxidation state of the carbon atoms where the new C=C double bond is formed is increased by +1. At the same time, the hydrogen acceptor is reduced as discussed below. The resulting diene can cyclize to form a six-membered ring, *e.g.* cyclohexene, which can be subsequently oxidized to aromatics through further HT processes.[35]

It is generally believed that HT processes leading to diene formation constitute key steps of aromatic formation.[4,8] Scheme 1 shows a general overview over the formation of an aromatic starting from an olefin. We have chosen benzene as the main example for simplicity. Nevertheless, it is known that methylated benzenes are typically more stable, depending on the zeotype, for example hexamethylbenzene and the heptamethyl benzylium cation in H-SSZ-13 and H-SAPO-34.[38] After isomerization, a terminal diene can, catalyzed by a BAS, form a C–C bond to give a cyclic olefin. This corresponds to a dimerization of olefins and the corresponding reverse reaction, olefin cracking. A potential alternative would also be the formation of a cycloalkane from an olefin. However, here it is difficult to envision a viable reaction mechanism. The reverse reaction would correspond to alkane cracking, which is known to proceed with high barriers and thus requires higher temperatures.[39]

There is an ongoing debate as to the molecules that serve as hydrogen acceptors.[29,40] Key observations are that while typically only little H_2 is formed, shorter alkanes are often found, the amount and ratio of which depend on reaction conditions.[15] Methane is the only alkane that can be formed directly from a HT to methanol or a surface methoxy species (SMS), whereas all other alkanes require HT to an olefin. Recently, other hydrogen acceptors have been suggested, and here in particular formaldehyde, which has been reported to be formed on Lewis acid sites (LAS) through the reaction of methanol with an olefin.[29,40] Recent work from our group substantiated this claim and showed that the oxidation of methanol to formaldehyde preferentially occurs on LAS.[41] Formaldehyde can subsequently react through a Prins type reaction to form a homoallylic alcohol, which can be easily dehydrated to form the corresponding diene.[42]

Herein, we systematically compare the formation of butadiene through reaction with formaldehyde as well as through other HT processes. We show how formed dienes can be methylated and isomerize to C_6–C_8 precursors that can cyclize to (substituted) cyclohexenes, which are subsequently being oxidized to (substituted) benzenes through ongoing HT processes. Our analysis is based on density functional theory (DFT) calculations employing Brønsted acidic H-SSZ-13. We note that, while other zeolites often display an acidity roughly within the range discussed here, other zeotypes (*e.g.* the CHA analogue H-SAPO-34) are usually much less acidic[43] which might alter preferred pathways and thus the formation process of aromatics discussed herein.

Methodology

DFT calculations and the computational model for H-SSZ-13 are analogous to previous works.[44] Briefly, we employed the acidic H-SSZ-13 zeolite and thus the chabazite (CHA) structure, with optimized lattice constants of $a = b = 13.625$ Å and $c = 15.067$ Å.[45] Our model contains a 1 × 1 × 1 CHA supercell with one silicon being replaced by aluminum and thus a Si/Al ratio of 35 and one proton per unit cell. DFT calculations were performed using the Vienna *ab initio* simulation package (VASP) in version 6.4.3[46,47] in the Atomic Simulation Environment (ASE).[48] The projector-augmented wave method[49] with one *k*-point sampling at the Γ-point only was employed. All structures were optimized using the PBE functional[50] with Grimme's D3 dispersion correction[51] (zero damping) (PBE-D3). Standard PAW potentials, a plane wave basis set with an energy cutoff of 400 eV, a Gaussian smearing width of 0.1 eV and a convergence criterion of 0.001 eV Å^{-1} were used. Transition states were calculated using the automated relaxed potential surface scan (ARPESS) method,[52] whose nature have been verified through the existence of a single imaginary frequency. Vibrational analysis was performed by calculating a partial Hessian that included the adsorbate and the acid site consisting of the proton, the corresponding oxygen and the adjacent Si and Al atom, with an atomic displacement of 0.01 Å. Since low harmonic frequencies lead to large errors in free energy calculations, we raised the vibrations below 12 cm^{-1} to this value.[53]

Since DFT calculations employing the PBE-D3 functional underestimate energy barriers related to the MTO process in zeotypes by an average of 50 kJ mol^{-1},[54,55] all energies were corrected by single-point calculations employing the ωB97M functional[56] with D4-corrections[57,58] (ωB97M-D4), as implemented in a local VASP version, as this functional has been shown to perform best in a recent benchmark study, with mean absolute errors well below 8 kJ mol^{-1}.[59]

Results

Olefin oxidation to dienes

We recently showed that LAS at surfaces of H-SSZ-13 can catalyze the HT between methanol and an olefin to yield formaldehyde and the corresponding hydrocarbon with free energy barriers (at 400 °C) being as low as 178 kJ mol^{-1} in case of iso-butene as the hydrogen acceptor.[41] Formaldehyde has been calculated to react rather easily at BAS of H-SSZ-13 to form allylic alcohols that dehydrate to the corresponding diene, confirming both the role of formaldehyde and LAS ascribed through extensive experiments recently.[29,40] We will now compare this reaction pathway to other HT reactions. We have conducted a systematic study of these using 2-butene as the olefin that is oxidized to butadiene in order to simplify our analysis. As the hydrogen acceptors we investigated methanol (MeOH) dimethyl ether (DME), formaldehyde (FA), ethene, propene and iso-butene as well as

hydrogen acceptors that are strongly bound to the acid site, such as surface methoxy species (SMS) and surface ethoxy species (SES) and lastly also the acid site (ZOH) itself (see Table 1 for results with 2-butene, Fig. 1 gives an overview of the reaction between 3-hexene and a SMS). While HT to alkenes and SES leads to the formation of alkanes, HT to SMS and ZOH yield methane and hydrogen, respectively. Table 1 reports the apparent free energies, meaning the free energy of the transition states of the HT reactions relative to 2-butene and the corresponding HT acceptor in the gas phase (or adsorbed in the case of SMS and SES). In general, we determine apparent free energies as the energetic span[60] in terms of Gibbs free energy. As can be seen from Table 1, all HT reactions exhibit rather high transition states with all of them being >210 kJ mol^{-1}, with the reaction SES + 2-butene → ethane + butadiene (barrier of 212 kJ mol^{-1}), HT to FA (213 kJ mol^{-1}) and a SMS (216 kJ mol^{-1}) constituting the lowest barriers. This compares with 178 kJ mol^{-1} for the oxidation of methanol to FA over LAS followed by the Prins reaction between 2-butene and FA forming *n*-pentadiene in bulk H-SSZ-13.[41] Hence, butadiene formation *via* the FA–LAS pathway has barriers that are substantially lower than all herein investigated HT reactions, highlighting the role that FA and LAS are ascribed to for the formation of dienes.

We also investigated the oxidation of longer chain olefins using a SMS as the HT acceptor, with all reaction free energy barriers referenced to the olefin in the gas phase as adsorption is usually uphill in free energy (see Fig. 1). Interestingly, the oxidation of longer chain olefins *via* HT to a SMS is more favorable than what is found for 2-butene, with barriers being between 180–200 kJ mol^{-1}, compared to 216 kJ mol^{-1} for 2-butene. However, one has to be careful as to what is used as the reference state. While SMS formation itself has a barrier of 172 kJ mol^{-1} when measured relative to methanol in the gas-phase, this barrier may increase in case that olefins are co-adsorbed at the acid site (*e.g.* 188 kJ mol^{-1} with co-adsorbed hexene, see Fig. 1). Nevertheless, judging from the data shown in Fig. 1, it seems plausible that the most efficient pathway towards dienes lies in the oxidation of longer chain olefins, especially in the absence of the FA–LAS pathway.

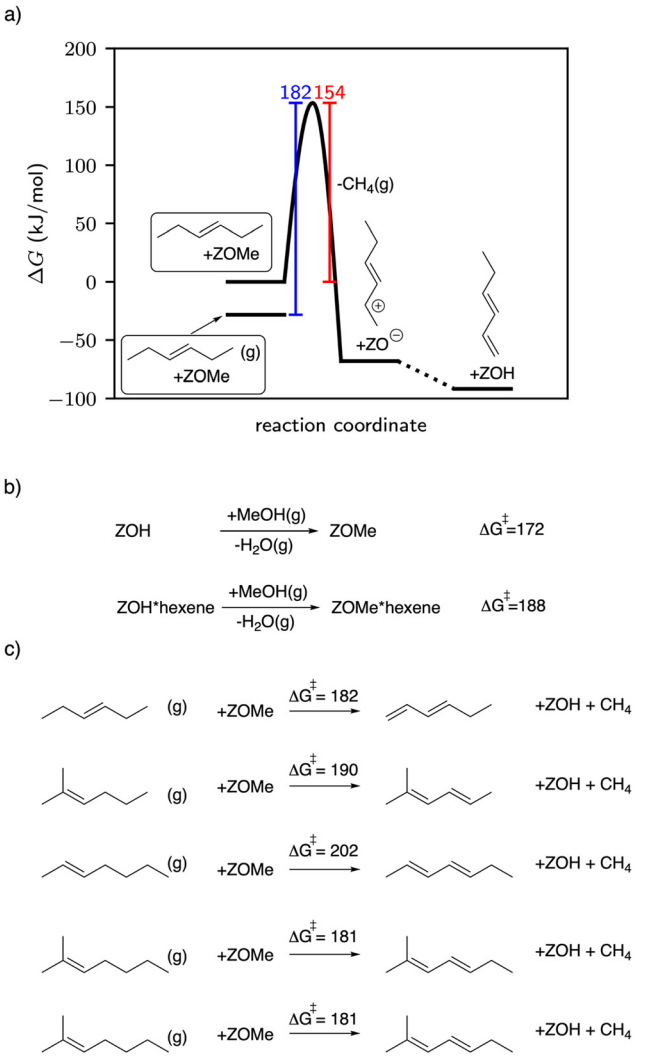

Fig. 1 (a) Free energy profile of the oxidation of 3-hexene to 1,3-hexadiene *via* HT to a SMS at 673 K and a pressure of 1 bar. Free energies are referenced to adsorbed 3-hexene, but the apparent activation free energy with respect to 3-hexene(g) is also shown. (b) Schematics showing the free energy barriers for the formation of a SMS from methanol both with an empty acid site (ZOH) and at an acid site with co-adsorbed hexene (ZOH*hexene). (c) Oxidation of 3-hexene, 2-methyl-2-hexene, 2-heptene, and 2-methyl-2-heptene *via* HT to a SMS with apparent activation free energies. All free energies are given in kJ mol^{-1}.

Table 1 Apparent activation free energies for hydride transfer from 2-butene to various acceptors X, resulting in the formation of butadiene and XH_2. All free energy barriers are relative to the zeolite and the corresponding molecules in the gas-phase and are given at 673 K, a reference pressure of 1 bar and in kJ mol^{-1}

X	XH_2	$\Delta G^{\ddagger}_{app}$
ZOH	ZOH + H_2	254
ZOMe (SMS)	ZOH + CH_4	216
ZOEt (SES)	ZOH + ethane	212
ZOH + MeOH	ZOH + H_2O + CH_4	292
ZOH + DME	ZOH + MeOH + CH_4	304
ZOH + formaldehyde	ZOH + MeOH	213
ZOH + ethylene	ZOH + ethane	240
ZOH + propylene	ZOH + propane	251
ZOH + isobutene	ZOH + isobutane	223

Diene methylation reactions

The previous section explored possible pathways for diene formation, both for the reaction producing butadiene, but also for the oxidation of higher olefins to produce longer chain dienes. In case that *e.g.* only butadiene is formed, this still needs to be converted to longer chain dienes before cyclization can take place. We will now show how butadiene can be methylated to longer chain dienes, exemplified by the reaction sequence from butadiene over pentadiene to hexadiene. Free energies are given relative to butadiene as well as MeOH in the gas phase. As can be seen from Fig. 2, both methylations proceed rather easily with free energy

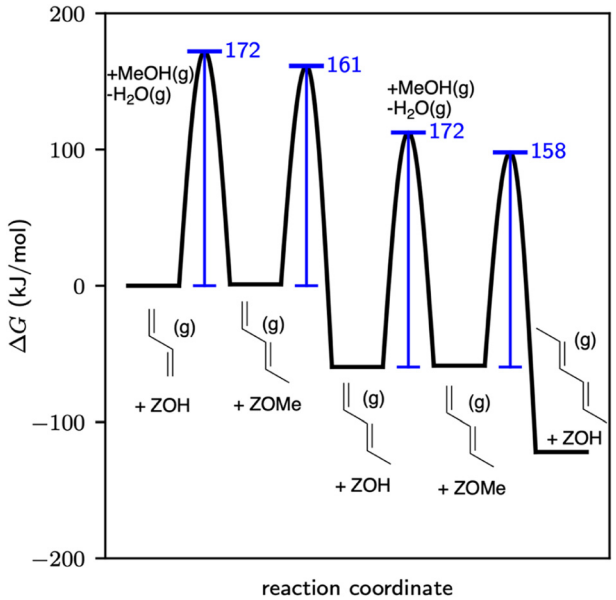

Fig. 2 Free energy profile of the methylation of butadiene to pentadiene and pentadiene to hexadiene *via* a SMS at 673 K and a pressure of 1 bar for all molecules. Note, that references are given to the dienes in the gas-phase. All free energies are given in kJ mol^{-1}.

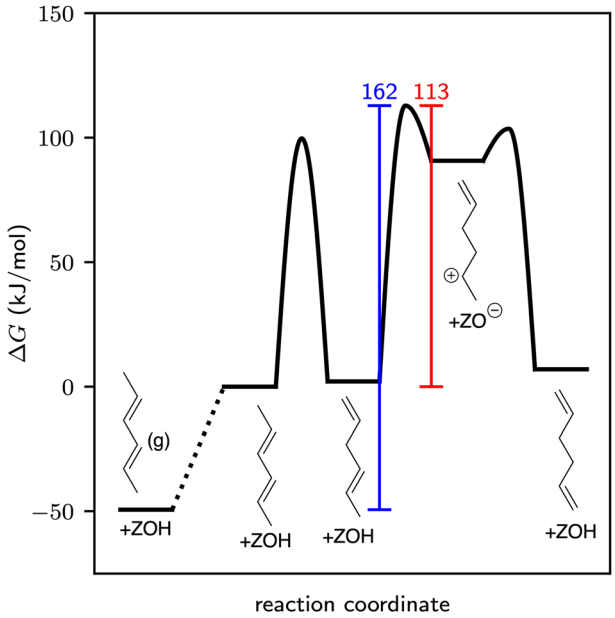

Fig. 3 Calculated free energy diagram for the isomerization of 2,4-hexadiene to 1,5-hexadiene over H-SSZ-13, relative to gas-phase (blue barrier) and adsorbed 2,4-hexadiene (red barrier) at 673 K and pressures of 1 bar for all molecules. All energies in kJ mol^{-1}.

barriers of about 160–170 kJ mol^{-1}, when referenced to the diene and a SMS, similar to methylation barriers of alkenes (see SI, Table S9).[61] Note that the formation of a SMS is 172 kJ mol^{-1} (see above), and thus similar in terms of barrier height.

Isomerization of hexadiene

The next step in this process is the isomerization of the double bond of the dienes. Since the conjugated dienes are more stable, as a first step in this process, the double bond of the diene needs to shift twice such that 1,5-dienes form. We have investigated this for the case of hexadiene, that is the reaction sequence from 2,4-hexadiene to 1,4-hexadiene to 1,5-hexadiene, see Fig. 3. These isomerizations proceed with comparatively low free energy barriers, with the highest identified for hexadiene being 162 kJ mol^{-1}, when measured to the diene in the gas-phase and an isolated acid site. Isomerization is uphill by about 7 kJ mol^{-1} in the case of adsorbed 2,4-hexadiene to adsorbed 1,5-hexadiene, due to the more stable double bond in the conjugated 2,4-hexadiene.

Cyclization of dienes

Next, we investigated five cyclization reactions of C_6–C_8 dienes. This is exemplarily shown for the cyclization of 2,4-hexadiene and 2,4-heptadiene in Fig. 4. While the barriers associated with the actual cyclization are rather small (111 and 66 kJ mol^{-1} for the isomers 1,5-hexadiene and 1,6-heptadiene, respectively), we note that these dienes do not correspond to the most stable state. If referenced to the most stable dienes in the gas phase (see also Fig. 3 for the stability and isomerization of hexadiene), these barriers increase by 60–70 kJ mol^{-1}. Still, barriers for cyclization of longer chain dienes are rather small in comparison. Notably, there is a large difference between the barriers for cyclization if the double bond attacks a secondary double bond as in the case of 1,6-heptadiene. In this case barriers are significantly smaller. This is also shown in Table 2 that lists the five cyclization barriers investigated herein, all of which are referenced to the most stable conjugated dienes. Whereas cyclization barriers for 2,4-hexadiene (*via* 1,5-hexadiene) and 2-methyl-2,4-hexadiene (*via* 2-methyl-1,5-hexadiene) are associated with barriers of about 180 kJ mol^{-1}, barriers for the cyclization involving a secondary carbon (*e.g.* for 2,4-heptadiene) are significantly lower at about 120 kJ mol^{-1} (with isomers being 106, 119, 125 kJ mol^{-1}).

Oxidation of cyclohexene

Lastly, (methylated) cyclohexenes can be oxidized to form (methylated) cyclohexadienes and finally (methylated) benzenes. Again, the oxidation occurs *via* HT steps that can proceed in combination with a large number of hydrogen acceptors. Here, we calculated these steps using HT from the cyclic compounds to a SMS (see Table 2 and Fig. 5). One possible path is shown exemplarily in Fig. 5, namely the oxidation of cyclohexene to benzene *via* two HT steps using SMS as the hydrogen acceptor, thus producing two molecules of methane. As can be seen from Fig. 5, the reaction barriers are quite feasible being 153 and 159 kJ mol^{-1} when measured to the corresponding adsorbed reactant and the SMS. Importantly, both HT reactions are very exergonic by −102 and −255 kJ mol^{-1}, with the overall reaction free energy from

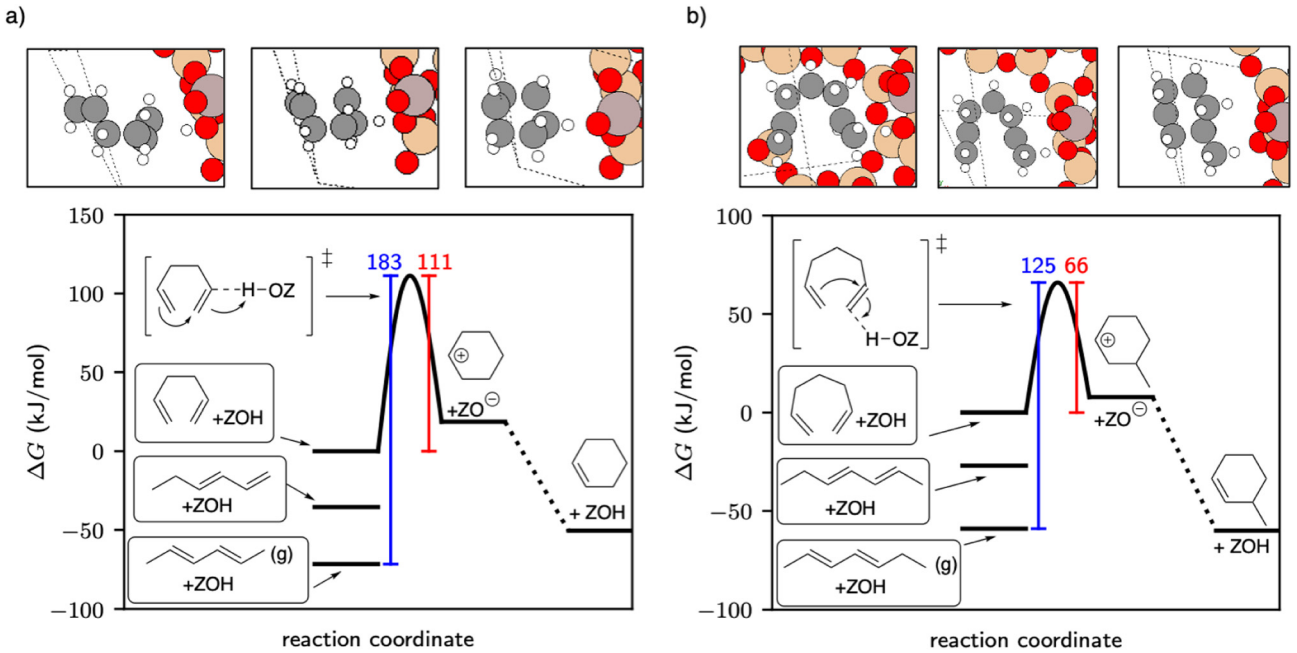

Fig. 4 Calculated free energy diagram of the cyclization of (a) 2,4-hexadiene and (b) 2,4-heptadiene. Free energies are shown starting with 2,4-hexadiene and 2,4-heptadiene in the gas-phase. Two double bond isomerization reactions yield 1,5-hexadiene (see also Fig. 3) and 1,6-heptadiene. The cyclization barrier is shown to the latter (red barrier) as well as to the most stable conjugated dienes (blue barrier). After cyclization a cation is formed at the acid site, that can deprotonate to cyclohexene (a) and methyl-cyclohexene (b). All free energies are given at 673 K and a pressure of 1 bar and in kJ mol^{-1}. Images of the atomic structures for initial, transition and final state are shown above the free energy diagrams (color code: H: white, C: gray, O: red, Si: beige, Al: gray).

cyclohexene to benzene being −356 kJ mol^{-1} when measured to cyclohexene adsorbed at an acid site. It can hence be concluded that these reactions are basically non reversible, especially for the final oxidation step producing benzene. We find similar results for the other four cyclizations considered herein, see Tables 2 and S8.

Discussion

We have investigated the formation of benzenes *via* oxidation of olefins to dienes, cyclization of dienes and the consecutive oxidation of the resulting cyclohexenes. A simplified overall reaction scheme for the conversion of hexene to benzene *via* (1) oxidation, (2) consecutive isomerization, (3) cyclization and (4) oxidation is shown in Fig. 6, where only the rate

Table 2 Overview over apparent activation free energies for the most relevant hydrogen transfer and cyclization transition states for various olefins. HT2 and HT3 show the maximum of the barriers for the formation of SMS and hydride transfer to SMS, see Table S8

Reaction/transition state	$\Delta G^{\ddagger}_{app}$ in kJ mol^{-1}		
	cyc	HT2	HT3
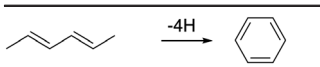	183	153	160
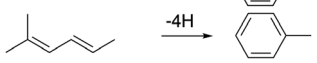	179	156	147
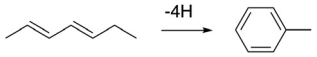	125	156	147
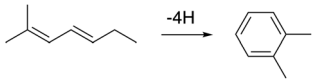	106	179	151
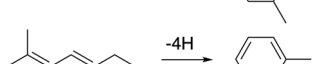	119	168	155

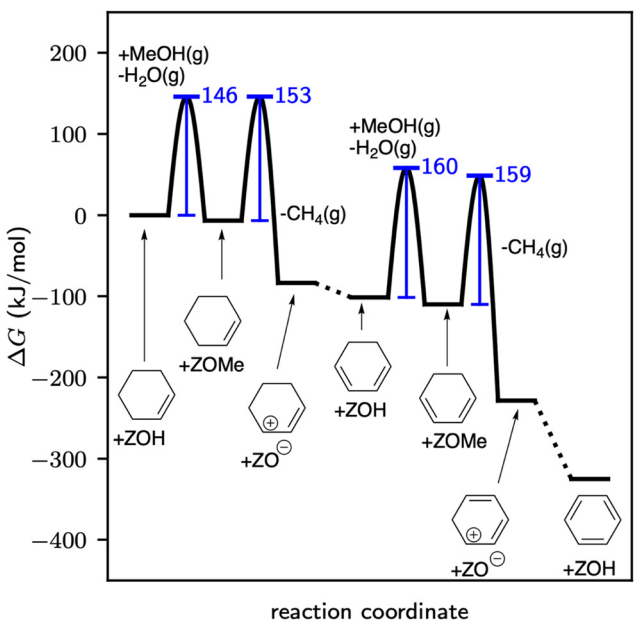

Fig. 5 Calculated free energy diagram of the oxidation of cyclohexene to benzene through a SMS referenced to methanol in the gas-phase. All free energies are given at 673 K and a pressure of 1 bar and in kJ mol^{-1}.

determining barriers are shown for each of these reaction steps. The overall oxidation is strongly exothermic by about 400 kJ mol^{-1} if methanol is used as a hydrogen acceptor, thus producing methane. Interestingly, the cyclization itself is associated with rather low barriers, which decrease even more for 1,6-heptadiene as well as related dienes. The overall highest barriers in this reaction sequence are given by the first HT of 3-hexene to produce 1,3-hexadiene, with a free energy barrier of 182 kJ mol^{-1} as well as by the cyclization of 1,5-hexadiene when referenced to the more stable 2,4-hexadiene in the gas-phase (183 kJ mol^{-1}). Note, that HT reactions involving shorter chain olefins, such as butene are higher in free energy (>210 kJ mol^{-1}), unless they proceed *via* FA formation over LAS and the Prins reaction pathway which is also around 180 kJ mol^{-1}. Importantly, cyclization of longer chain dienes proceeds with substantially lower barrier than hexadiene, as exemplified for heptadiene (125 kJ mol^{-1}), which results in the formation of toluene.

We thus conclude that the formation of dienes is likely to constitute the rate determining steps of this overall reaction mechanism and that once dienes are formed, they are rather easily isomerized, cyclized and oxidized to the corresponding aromatics, a reaction that is so exothermic that it is basically irreversible.

Since the oxidation of C_{6+} olefins constitutes the rate determining step for the formation of aromatics, the stability of these olefins with respect to either further methylation and/or cracking compared to oxidation is likely deciding whether they form aromatics or continue within the olefin cycle. It is thus of interest to compare cracking barriers for longer chain olefins with respect to the rate determining step of the cyclization reaction. Scheme 2 shows the calculated free energy barriers for cracking of 2,4-dimethyl-2-pentene, 2,2-dimethyl-3-pentene, 2-methyl-3-hexene, 3-methyl-3-hexene, 2-methyl-2-pentene and 3-hexene that have been reported elsewhere,[61] corrected here using the same computational methodology. Interestingly, free energy

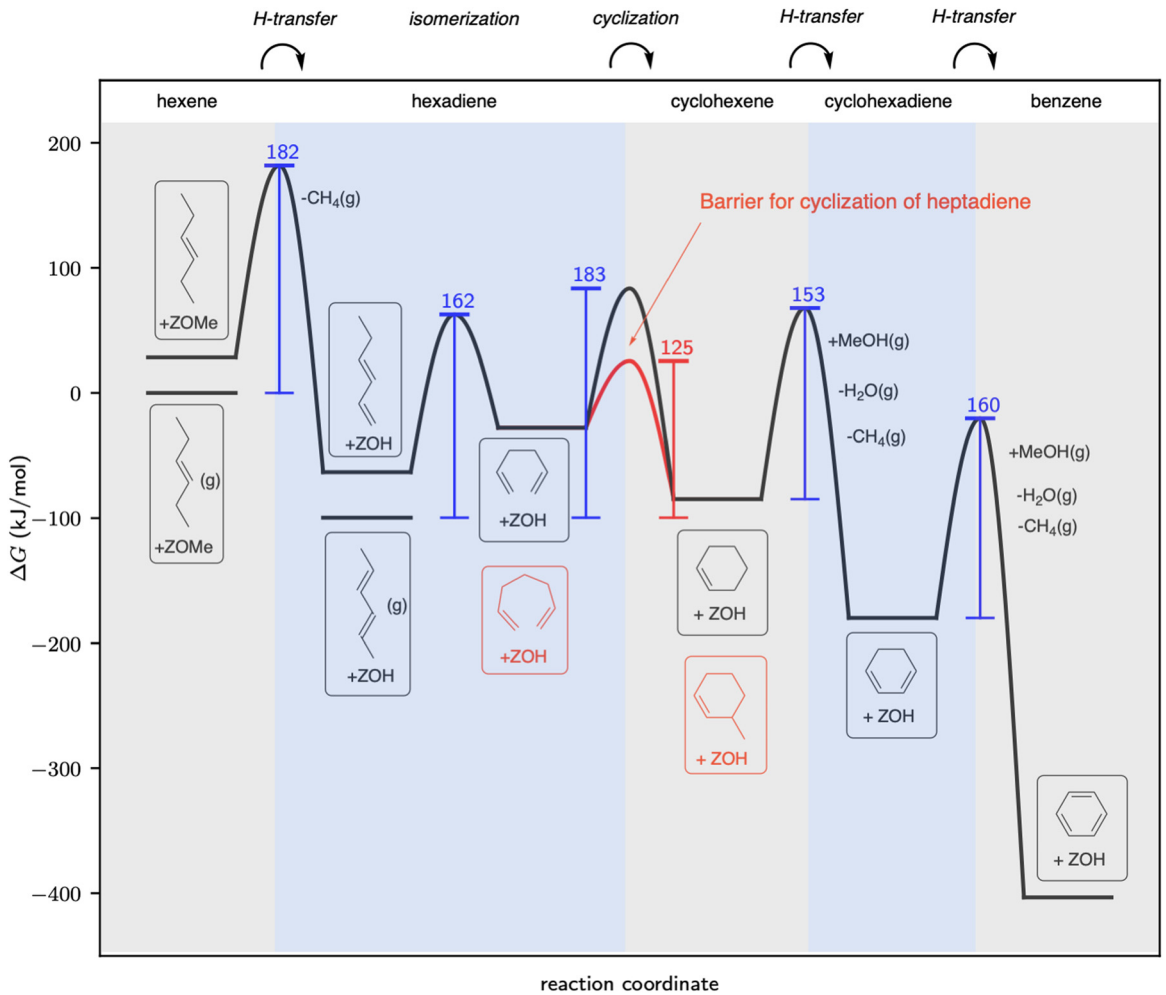

Fig. 6 Calculated Gibbs free energy diagram for a simplified mechanism of the H-SSZ-13 catalyzed formation of benzene with 3-hexene as the starting point. The difference in barriers for cyclization is indicated for 1,6-heptadiene in red, as compared to 1,5-hexadiene (in black). The shaded areas correspond to hexene, hexadiene, cyclohexene, cyclohexadiene and benzene, connected by the distinct reaction steps in this mechanism, being (1) oxidation, (2) isomerization, (3) cyclization and (4) oxidation. All free energies are given relative to 3-hexene in the gas phase, at 673 K and a pressure of 1 bar and are given in kJ mol^{-1}.

barriers range from 130–195 kJ mol^{-1}, depending on the reacting olefin. As expected, more branched olefins are calculated to have lower barriers as they form more stable secondary and tertiary cations in the transition state. Less branched, linear olefins have cracking barriers that are comparable to those for HT reactions, *e.g.* 3-hexene, that has a cracking barrier of 174 kJ mol^{-1}, compared to a HT barrier of 182 kJ mol^{-1} when using a SMS as the HT acceptor. Whether olefins are being cracked or oxidized will thus depend on the degree of branching, but also on the availability of suitable HT acceptors, and would likely require elaborate kinetic models to be solved. Once cracked into shorter olefins, these can diffuse out of the zeolite and leave as products of the process. Alternatively, they can further react by repeated methylation or dimerization and could thus again become reactants for cyclization and the formation of aromatics.

We have primarily focused in this work on the formation of dienes through hydrogen transfer from the olefin to an acceptor. However, as already mentioned, diene formation can also occur through a Prins reaction that couples formaldehyde and an olefin to form a diene after subsequent water elimination. The formation of formaldehyde itself is believed to be the main bottleneck in this reaction and has been the focus of many investigations.[31,41,62–64] The pronounced effect of co-feeding formaldehyde has been demonstrated in experimental studies.[65,66]

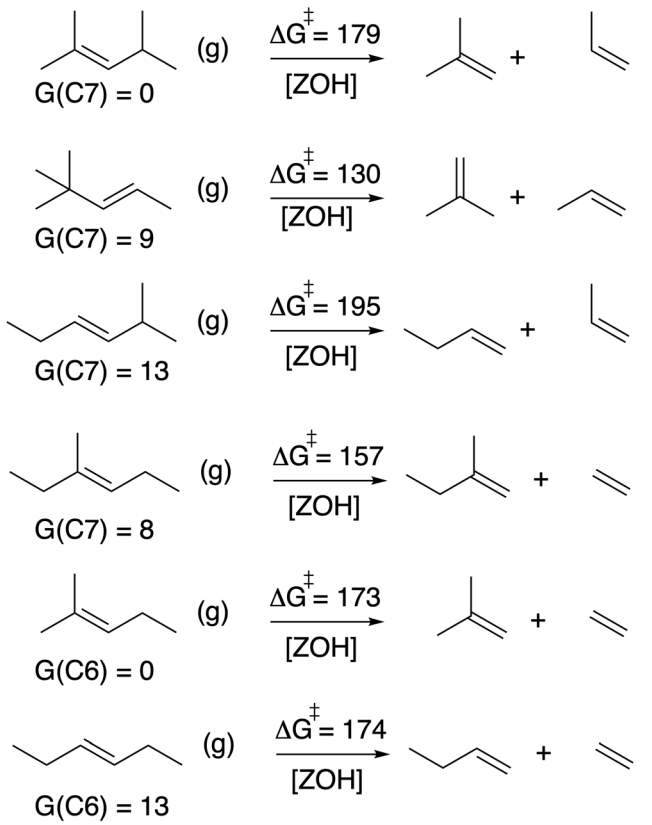

Scheme 2 Calculated free energy barriers for cracking of 2,4-dimethyl-2-pentene, 2,2-dimethyl-3-pentene, 2-methyl-3-hexene, 3-methyl-3-hexene, 2-methyl-2-pentene and 3-hexene. Data has been taken from previous work,[61] but was recomputed here with single point calculations using ωB97M-D4 to give a fully consistent treatment. All free energies are given relative to the depicted olefin in the gas-phase, at 673 K, a pressure of 1 bar and in kJ mol^{-1}. The relative stability of the olefins is given relative to the most stable isomer with the same number of atoms, *i.e.* six or seven carbon atoms, which is set to zero, *G*(C6) = 0 and *G*(C7) = 0, respectively.

Conclusion

We have presented a theoretical study of the reaction mechanism of olefin oxidation and cyclization to produce aromatics over a computational model of Brønsted acidic H-SSZ-13. Our calculations indicate that the first HT step to produce a diene is likely to constitute the rate determining step of the overall reaction cycle. Given, that the overall reaction to the final methyl benzenes is highly exothermic, aromatics are formed irreversibly once the reaction produces dienes. The key step in terms of selectivity of olefins towards aromatics formation is thus likely given by the competition between HT of an olefin to a hydrogen acceptor such as methanol or a SMS and reaction of the olefin either through further methylation or cracking. We investigated this exemplarily for a subset of branched and linear olefin isomers that are calculated to be particularly stable in free energy and find that, while cracking barriers of branched olefins are generally lower, barriers for the cracking of linear olefins have similar values compared to HT reactions, in the case of H-SSZ-13. The degree to which olefins that are repeatedly formed in the olefin cycle are being oxidized and thus fed into the formation of aromatics seems to depend primarily on the formed olefin and the availability of suitable hydrogen acceptors. A more conclusive in-depth investigation of this, however, would require elaborate kinetic models.

Conflicts of interest

There are no conflicts to declare.

Data availability

All data supporting this study are provided as part of the main manuscript and the accompanying supplementary information (SI).

Supplementary information is available. See DOI: https://doi.org/10.1039/d6cy00727a.

Acknowledgements

The authors acknowledge support by the state of Baden-Württemberg through bwHPC (bwunicluster and JUSTUS, RVbw17D011) and the German Research Foundation (DFG) through grant no. INST40/575-1FUGG (JUSTUS2cluster). Financial support from the Helmholtz Association is also gratefully acknowledged.

References

1 M. Stöcker, Methanol-to-hydrocarbons: catalytic materials and their behavior, *Microporous Mesoporous Mater.*, 1999, **29**(1–2), 3–48, DOI: 10.1039/d5se00231a.

2 J. F. Haw, W. Song, D. M. Marcus and J. B. Nicholas, The Mechanism of Methanol to Hydrocarbon Catalysis, *Acc. Chem. Res.*, 2003, **36**, 317–326, DOI: 10.1021/ar020006o.

3 U. Olsbye, S. Svelle, M. Bjørgen, P. Beato, T. V. W. Janssens, F. Joensen, S. Bordiga and K. P. Lillerud, Conversion of Methanol to Hydrocarbons: How Zeolite Cavity and Pore Size Controls Product Selectivity, *Angew. Chem., Int. Ed.*, 2012, **51**, 5810–5831, DOI: 10.1002/anie.201103657.

4 S. Ilias and A. Bhan, Mechanism of the Catalytic Conversion of Methanol to Hydrocarbons, *ACS Catal.*, 2013, **3**, 18–31, DOI: 10.1021/cs3006583.

5 P. Tian, Y. Wei, M. Ye and Z. Liu, Methanol to Olefins (MTO): From Fundamentals to Commercialization, *ACS Catal.*, 2015, **5**, 1922–1938, DOI: 10.1021/acscatal.5b00007.

6 I. Yarulina, A. D. Chowdhury, F. Meirer, B. M. Weckhuysen and J. Gascon, Recent trends and fundamental insights in the methanol-to-hydrocarbons process, *Nat. Catal.*, 2018, **1**, 398–411, DOI: 10.1038/s41929-018-0078-5.

7 B. J. M. Etzold, M. Hungsberg, M. Ebrahim-Moghaddam, F. Herold, N. Dahmen and F. Studt, Energy Requirements for Sustainable Olefin Production From CO2 via Electro- or Thermal Catalysis, *Chem. Eng. Technol.*, 2025, **48**, e70034, DOI: 10.1002/ceat.70034.

8 T. Li, T. Shoinkhorova, J. Gascon and J. Ruiz-Martínez, Aromatics Production via Methanol-Mediated Transformation Routes, *ACS Catal.*, 2021, **11**, 7780–7819, DOI: 10.1021/acscatal.1c01422.

9 A. Li, J. Zheng, Z. Wang and Z. Zhang, Research advances and future perspectives in Fischer–Tropsch synthesis for sustainable aviation fuel, *Sustainable Energy Fuels*, 2026, **10**, 42–55, DOI: 10.1039/D5SE01412C.

10 I. M. Dahl and S. Kolboe, On the Reaction-Mechanism for Propene Formation in the Mto Reaction over Sapo-34, *Catal. Lett.*, 1993, **20**, 329–336.

11 I. M. Dahl and S. Kolboe, On the Reaction Mechanism for Hydrocarbon Formation from Methanol over SAPO-34: I. Isotopic Labeling Studies of the Co-Reaction of Ethene and Methanol, *J. Catal.*, 1994, **149**, 458–464.

12 I. M. Dahl and S. Kolboe, On the reaction mechanism for hydrocarbon formation from methanol over SAPO-34. 2. Isotopic labeling studies of the co-reaction of propene and methanol, *J. Catal.*, 1996, **161**, 304–309.

13 D. Chen, H. P. Rebo, K. Moljord and A. Holmen, Influence of Coke Deposition on Selectivity in Zeolite Catalysis, *Ind. Eng. Chem. Res.*, 1997, **36**, 3473–3479, DOI: 10.1021/ie9700223.

14 T. V. W. Janssens, S. Svelle and U. Olsbye, Kinetic modeling of deactivation profiles in the methanol-to-hydrocarbons (MTH) reaction: A combined autocatalytic–hydrocarbon pool approach, *J. Catal.*, 2013, **308**, 122–130.

15 J. S. Martinez-Espin, M. Mortén, T. V. W. Janssens, S. Svelle, P. Beato and U. Olsbye, New insights into catalyst deactivation and product distribution of zeolites in the methanol-to-hydrocarbons (MTH) reaction with methanol and dimethyl ether feeds, *Catal. Sci. Technol.*, 2017, **7**, 2700–2716.

16 D. Rojo-Gama, M. Nielsen, D. S. Wragg, M. Dyballa, J. Holzinger, H. Falsig, L. F. Lundegaard, P. Beato, R. Y. Brogaard, K. P. Lillerud, U. Olsbye and S. Svelle, A Straightforward Descriptor for the Deactivation of Zeolite Catalyst H-ZSM-5, *ACS Catal.*, 2017, **7**, 8235–8246.

17 D. Rojo-Gama, L. Mentel, G. N. Kalantzopoulos, D. K. Pappas, I. Dovgaliuk, U. Olsbye, K. P. Lillerud, P. Beato, L. F. Lundegaard, D. S. Wragg and S. Svelle, Deactivation of Zeolite Catalyst H-ZSM-5 during Conversion of Methanol to Gasoline: Operando Time- and Space-Resolved X-ray Diffraction, *J. Phys. Chem. Lett.*, 2018, **9**, 1324–1328.

18 A. E. Enss, P. N. Plessow and F. Studt, A computational study on the formation mechanism of naphthalenic species under MTO conditions in H-SSZ-13, *Catal. Sci. Technol.*, 2025, **15**, 7200, DOI: 10.1039/d5cy00837a.

19 M. Bjørgen, U. Olsbye, D. Petersen and S. Kolboe, The methanol-to-hydrocarbons reaction: insight into the reaction mechanism from [12C]benzene and [13C]methanol coreactions over zeolite H-beta, *J. Catal.*, 2004, **221**, 1–10, DOI: 10.1016/S0021-9517(03)00284-7.

20 S. Svelle, S. Kolboe, O. Swang and U. Olsbye, Methylation of Alkenes and Methylbenzenes by Dimethyl Ether or Methanol on Acidic Zeolites, *J. Phys. Chem. B*, 2005, **109**, 12874–12878, DOI: 10.1021/jp051125z.

21 S. Svelle, F. Joensen, J. Nerlov, U. Olsbye, K. P. Lillerud, S. Kolboe and M. Bjorgen, Conversion of Methanol into Hydrocarbons over Zeolite H-ZSM-5: Ethene Formation Is Mechanistically Separated from the Formation of Higher Alkenes, *J. Am. Chem. Soc.*, 2006, **128**, 14770–14771, DOI: 10.1021/ja065810a.

22 D. M. McCann, D. Lesthaeghe, P. W. Kletnieks, D. R. Guenther, M. J. Hayman, V. Van Speybroeck, M. Waroquier and J. F. Haw, A Complete Catalytic Cycle for Supramolecular Methanol-to-Olefins Conversion by Linking Theory with Experiment, *Angew. Chem.*, 2008, **120**, 5257–5260, DOI: 10.1002/ange.200705453.

23 Q. Y. Qian, C. Vogt, M. Mokhtar, A. M. Asiri, S. A. Al-Thabaiti, S. N. Basahel, J. Ruiz-Martinez and B. M. Weckhuysen, Combined Operando UV/Vis/IR Spectroscopy Reveals the Role of Methoxy and Aromatic Species during the Methanol-to-Olefins Reaction over H-SAPO-34, *ChemCatChem*, 2014, **6**, 3396–3408, DOI: 10.1002/cctc.201402714.

24 C. M. Wang, Y. D. Wang, Y. J. Du, G. Yang and Z. K. Xie, Similarities and differences between aromatic-based and olefin-based cycles in H-SAPO-34 and H-SSZ-13 for methanol-to-olefins conversion: insights from energetic span model, *Catal. Sci. Technol.*, 2015, **5**, 4354–4364, DOI: 10.1039/C5CY00483G.

25 K. De Wispelaere, J. S. Martínez-Espín, M. J. Hoffmann, S. Svelle, U. Olsbye and T. Bligaard, Understanding zeolite-catalyzed benzene methylation reactions by methanol and dimethyl ether at operating conditions from first principle

microkinetic modeling and experiments, *Catal. Today*, 2018, **312**, 35–43, DOI: 10.1016/j.cattod.2018.02.042.

26 X. Wang, C. Wang, Y. Chu, Y. Liu, M. Hu, F. Deng, J. Xu and J. Yu, Deciphering the Link between Zeolite Crystal Size, Brønsted Acid Site Distribution, and Dual-Cycle Selectivity in Methanol-to-Olefins over Zeolite, *ACS Catal.*, 2024, **14**, 15609–15621, DOI: 10.1021/acscatal.4c05555.

27 L. Maggiulli, V. L. Sushkevich, A. E. Enss, F. Studt, J. A. van Bokhoven and D. Ferri, Influence of the Acid Reactivity of Carbenium Ions in Zeolites on the Methanol-to-Olefins Process, *Angew. Chem., Int. Ed.*, 2025, **64**, e202514759.

28 X. Sun, S. Mueller, H. Shi, G. L. Haller, M. Sanchez-Sanchez, A. C. van Veen and J. A. Lercher, On the impact of co-feeding aromatics and olefins for the methanol-to-olefins reaction on HZSM-5, *J. Catal.*, 2014, **314**, 21–31, DOI: 10.1016/j.jcat.2014.03.013.

29 S. Müller, Y. Liu, F. M. Kirchberger, M. Tonigold, M. Sanchez-Sanchez and J. A. Lercher, Hydrogen Transfer Pathways during Zeolite Catalyzed Methanol Conversion to Hydrocarbons, *J. Am. Chem. Soc.*, 2016, **138**, 15994–16003, DOI: 10.1021/jacs.6b09605.

30 E. Borodina, H. Sharbini Harun Kamaluddin, F. Meirer, M. Mokhtar, A. M. Asiri, S. A. Al-Thabaiti, S. N. Basahel, J. Ruiz-Martinez and B. M. Weckhuysen, Influence of the Reaction Temperature on the Nature of the Active and Deactivating Species During Methanol-to-Olefins Conversion over H-SAPO-34, *ACS Catal.*, 2017, **7**, 5268–5281, DOI: 10.1021/acscatal.7b01497.

31 L. Kilburn, M. DeLuca, A. J. Hoffman, S. Patel and D. Hibbitts, Comparing alkene-mediated and formaldehyde-mediated diene formation routes in methanol-to-olefins catalysis in MFI and CHA, *J. Catal.*, 2021, **400**, 124–139, DOI: 10.1016/j.jcat.2021.05.010.

32 M. Fecík, P. N. Plessow and F. Studt, Theoretical investigation on the side-chain mechanism of the MTO process over H-SSZ-13 using DFT and ab initio calculations, *Catal. Sci. Technol.*, 2021, **11**, 3826.

33 P. N. Plessow, A. E. Enss, P. Huber and F. Studt, A new mechanistic proposal for the aromatic cycle of the MTO process based on a computational investigation for H-SSZ-13, *Catal. Sci. Technol.*, 2022, **12**, 3516.

34 P. N. Plessow and F. Studt, Cooperative Effects of Active Sites in the MTO Process: A Computational Study of the Aromatic Cycle in H-SSZ-13, *ACS Catal.*, 2023, **13**, 624.

35 H. Montalvo-Castro, M. DeLuca, L. Kilburn and D. Hibbitts, Mechanisms and Kinetics of the Dehydrogenation of C6–C8 Cycloalkanes, Cycloalkenes, and Cyclodienes to Aromatics in H-MFI Zeolite Framework, *ACS Catal.*, 2023, **13**, 99–112, DOI: 10.1021/acscatal.2c03360.

36 A. E. Enss, P. N. Plessow and F. Studt, Theoretical investigation of the paring mechanism of the MTO process in different zeolites, *J. Catal.*, 2024, **432**, 115363, DOI: 10.1016/j.jcat.2024.115363.

37 Q. Chen, J. Liu and B. Yang, Deciphering the Diffusion-Improved Selectivity of Ethylene Mediated by the Mesoscale Spatial Pattern of Aromatics in Zeolite-Catalyzed Methanol-to-Olefin Processes, *JACS Au*, 2025, **5**, 1791–1802, DOI: 10.1021/jacsau.5c00045.

38 K. Skladanová, M. Gešvandtnerová, E. Sola, C. Chizallet, T. Pigeon, M. Badawi and T. Bučko, Isobutanol dehydration catalyzed by bridging OH groups at the (100) surface of ferrierite: From static DFT to machine learning accelerated molecular dynamics, *J. Catal.*, 2026, **461**, 117024, DOI: 10.1016/j.jcat.2026.117024.

39 F. Berger, M. Rybicki and J. Sauer, Adsorption and cracking of propane by zeolites of different pore size, *J. Catal.*, 2021, **395**, 117, DOI: 10.1016/j.jcat.2020.12.008.

40 Y. Liu, F. M. Kirchberger, S. Müller, M. Eder, M. Tonigold, M. Sanchez-Sanchez and J. A. Lercher, Critical role of formaldehyde during methanol conversion to hydrocarbons, *Nat. Commun.*, 2019, **10**, 1462.

41 A. E. Enss, P. Huber, P. N. Plessow and F. Studt, Methanol-Mediated Hydrogen Transfer Reactions at Surface Lewis Acid Sites of H-SSZ-13, *J. Phys. Chem. C*, 2024, **128**, 15367–15379, DOI: 10.1021/acs.jpcc.4c03408.

42 E. S. Vasiliadou, S. Li, S. Caratzoulas and R. F. Lobo, Formaldehyde-isobutene Prins condensation over MFI-type zeolites, *Catal. Sci. Technol.*, 2018, **8**, 5794–5806, DOI: 10.1021/acs.jpcc.4c03408.

43 C.-M. Wang, R. Y. Brogaard, B. M. Weckhuysen, J. K. Nørskov and F. Studt, Reactivity Descriptor in Solid Acid Catalysis: Predicting Turnover Frequencies for Propene Methylation in Zeotypes, *J. Phys. Chem. Lett.*, 2014, **5**, 1516, DOI: 10.1021/jz500482z.

44 H. Vicente, P. Huber, A. G. Gayubo, F. Studt and P. N. Plessow, Reactivity of pentamethylcyclopentenyl Cations toward Olefin Formation in the Methanol-to-Olefin (MTO) Process, *J. Phys. Chem. C*, 2025, **129**, 20971–20980, DOI: 10.1021/acs.jpcc.5c07265.

45 P. N. Plessow and F. Studt, Unraveling the Mechanism of the Initiation Reaction of the Methanol to Olefins Process Using ab Initio and DFT Calculations, *ACS Catal.*, 2017, **7**, 7987–7994, DOI: 10.1021/acscatal.7b03114.

46 G. Kresse and J. Furthmüller, Efficient iterative schemes for ab initio total-energy calculations using a plane-wave basis set, *Phys. Rev. B: Condens. Matter Mater. Phys.*, 1996, **54**, 11169–11186.

47 G. Kresse and D. Joubert, From ultrasoft pseudopotentials to the projector augmented-wave method, *Phys. Rev. B: Condens. Matter Mater. Phys.*, 1999, **59**, 1758–1775.

48 A. Hjorth Larsen, J. Jørgen Mortensen, J. Blomqvist, I. E. Castelli, R. Christensen, M. Dułak, J. Friis, M. N. Groves, B. Hammer, C. Hargus, E. D. Hermes, P. C. Jennings, P. Bjerre Jensen, J. Kermode, J. R. Kitchin, E. Leonhard Kolsbjerg, J. Kubal, K. Kaasbjerg, S. Lysgaard, J. Bergmann Maronsson, T. Maxson, T. Olsen, L. Pastewka, A. Peterson, C. Rostgaard, J. Schiøtz, O. Schütt, M. Strange, K. S. Thygesen, T. Vegge, L. Vilhelmsen, M. Walter, Z. Zeng and K. W. Jacobsen, *J. Phys.: Condens. Matter*, 2017, **29**, 273002.

49 P. E. Blöchl, Projector augmented-wave method, *Phys. Rev. B: Condens. Matter Mater. Phys.*, 1994, **50**, 17953–17979.

50 J. P. Perdew, K. Burke and M. Ernzerhof, Generalized Gradient Approximation Made Simple, *Phys. Rev. Lett.*, 1996, **77**, 3865–3868.

51 S. Grimme, J. Antony, S. Ehrlich and H. Krieg, A consistent and accurate ab initio parametrization of density functional dispersion correction (DFT-D) for the 94 elements H-Pu, *J. Chem. Phys.*, 2010, **132**, 154104.

52 P. N. Plessow, Efficient Transition State Optimization of Periodic Structures through Automated Relaxed Potential Energy Surface Scans, *J. Chem. Theory Comput.*, 2018, **14**, 981–990.

53 R. Y. Brogaard, R. Henry, Y. Schuurman, A. J. Medford, P. G. Moses, P. Beato, S. Svelle, J. K. Nørskov and U. Olsbye, Methanol-to-hydrocarbons conversion: The alkene methylation pathway, *J. Catal.*, 2014, **314**, 159–169, DOI: 10.1016/j.jcat.2014.04.006.

54 T. J. Goncalves, P. N. Plessow and F. Studt, On the Accuracy of Density Functional Theory in Zeolite Catalysis, *ChemCatChem*, 2019, **11**, 4368–4376, DOI: 10.1002/cctc.201900791.

55 P. N. Plessow and F. Studt, How Accurately Do Approximate Density Functionals Predict Trends in Acidic Zeolite Catalysis?, *J. Phys. Chem. Lett.*, 2020, **11**, 4305–4310, DOI: 10.1021/acs.jpclett.0c01240.

56 N. Mardirossian and M. Head-Gordon, ωB97M-V. A combinatorially optimized, range-separated hybrid, meta-GGA density functional with VV10 nonlocal correlation, *J. Chem. Phys.*, 2016, **144**, 214110.

57 A. Naji-Najibi and L. Goerigk, DFT-D4 counterparts of leading meta-generalized-gradient approximation and hybrid density functionals for energetics and geometries, *J. Comput. Chem.*, 2020, **41**, 2562–2572.

58 A. Najibi and L. Goerigk, The Nonlocal Kernel in van der Waals Density Functionals as an Additive Correction: An Extensive Analysis with Special Emphasis on the B97M-Vand ωB97M-V Approaches, *J. Chem. Theory Comput.*, 2018, **14**, 5725–5738.

59 P. Huber and P. N. Plessow, Accurate and Efficient Description of Acidic Zeolites with Plane-Wave Density Functional Theory Using Range-Separated Hybrid Functionals, *ChemPhysChem*, 2025, **26**, e202500147.

60 S. Kozuch and S. Shaik, How to Conceptualize Catalytic Cycles? The Energetic Span Model, *Acc. Chem. Res.*, 2011, **44**, 101, DOI: 10.1021/ar1000956.

61 P. N. Plessow and F. Studt, Olefin methylation and cracking reactions in H-SSZ-13 investigated with ab initio and DFT calculations, *Catal. Sci. Technol.*, 2018, **8**, 4420, DOI: 10.1039/c8cy01194j.

62 J. S. Martínez-Espín, K. De Wispelaere, T. V. W. Janssens, S. Svelle, K. P. Lillerud, P. Beato, V. Van Speybroeck and U. Olsbye, Hydrogen Transfer versus Methylation: On the Genesis of Aromatics Formation in the Methanol-To-Hydrocarbons Reaction over H-ZSM-5, *ACS Catal.*, 2017, **7**, 5773, DOI: 10.1021/acscatal.7b01643.

63 W. Chen, J. Sobalska, W. Fu, K. A. Tarach, M. Bocus, T. Tang, K. Góra-Marek and V. Van Speybroeck, Formaldehyde-Mediated Initial Carbon–Carbon Bond Formation in Zeolite-Catalyzed Methanol-to-Hydrocarbon Conversion, *J. Am. Chem. Soc.*, 2025, **147**, 24719, DOI: 10.1021/jacs.5c06141.

64 H. Vicente and P. N. Plessow, Formaldehyde formation and its impact on the MTO initiation investigated with ab initio molecular dynamics simulations, *J. Catal.*, 2026, **457**, 116817, DOI: 10.1016/j.jcat.2026.116817.

65 V. Paunović, X. Wu, L. Maggiulli, D. Ferri, P. Hemberger, A. Bodi and J. A. van Bokhoven, The formation, reactivity and transformation pathways of formaldehyde in the methanol-to-hydrocarbon conversion, *Catal. Sci. Technol.*, 2024, **14**, 1216, DOI: 10.1039/d3cy01786a.

66 B. L. Foley, B. A. Johnson and A. Bhan, Kinetic Evaluation of Deactivation Pathways in Methanol-to-Hydrocarbon Catalysis on HZSM-5 with Formaldehyde, Olefinic, Dieneic, and Aromatic Co-Feeds, *ACS Catal.*, 2021, **11**, 3628, DOI: 10.1021/acscatal.0c05335.

